SEMARAK ILMU PUBLISHING

Journal of Advanced Research in Fluid Mechanics and Thermal Sciences

Journal homepage:
https://semarakilmu.com.my/journals/index.php/fluid_mechanics_thermal_sciences/index
ISSN: 2289-7879

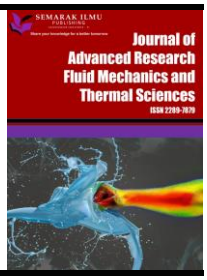

Feasibility of Pico Scale Turgo Turbine Blade Manufacturing Method Using Three-Dimension Printer Technology

Imam Syofii[1], Dewi Puspita Sari[1], Mochamad Amri Santosa[1], Suproyadi[2], Anthony Costa[3], Dendy Adanta[2,4,*], Rudi Darussalam[4], Andri Setiawan[4], Arifin Santosa[4], Kusnadi[4]

[1] Study Program of Mechanical Engineering Education, Faculty of Teacher Training and Education, Universitas Sriwijaya, Ogan Ilir – 30662, South Sumatera, Indonesia
[2] Department of Mechanical Engineering, Faculty of Engineering, Universitas Sriwijaya, Ogan Ilir – 30662, South Sumatera, Indonesia
[3] Department of Civil Engineering, Faculty of Engineering, Universitas Sriwijaya, Ogan Ilir – 30662, South Sumatera, Indonesia
[4] Research Center for Energy Conversion and Conservation, National Research and Innovation Agency (BRIN), Indonesia

ARTICLE INFO

Article history:
Received 26 February 2023
Received in revised form 4 June 2023
Accepted 11 June 2023
Available online 25 June 2023

Keywords:
Turgo turbine; triangle velocity; blade; 3D printer

ABSTRACT

This study proposed the design of pico-scale Turgo turbine blades using triangle velocity and printing blades using three-dimensional (3D) printer technology. Then, describe the testing method of Pico scale Turgo turbines in laboratory conditions. The velocity triangle analysis accommodates backflow where it is affected by blade angle; this is relevant to the Turgo turbine because the flow and blades have an angle so that the estimated change in momentum approaches real conditions. Based on calculation results, the geometry of the pico-scale Turgo turbine blades that produce maximum performance is as follows: angle of attack is 20°, inlet blade angle is 40°, outlet blade angle is 10°, and radius blade angle is 15°. Then, simulation results determine the potential water power that the blade is capable of receiving is 17.5 W. The experimental setup has a potential water power of 14.81 W, lower than the mechanical strength simulation results. From the experimental results, the performance maximum is 0.092; the average deviation between the analytical and experimental is 4%. Therefore, the manufacture of pico-scale Turgo turbine blades using 3D printer technology is considered because of the ease of the manufacturing process, the time needed in the manufacturing process is short, and the cost is low.

1. Introduction

The Turgo turbine is categorized as an impulse turbine, and the blades absorb the kinetic energy of the water into mechanical power [1]. The Turgo turbine is a development of the Pelton turbine, so its approaches are widely adapted using the Pelton turbine concept [2]. Turgo turbines are considered an alternative to independent power plants in remote areas because of their simple shape and easy maintenance and operation; it is the pico scale for remote areas [3-7].

Pico scale Turgo turbine research development continues so that it can be applied in low head conditions (<5 m). Williamson *et al.,* [8] recommend designing a Turgo turbine with a two-

* *Corresponding author.*
E-mail address: dendyadanta@ymail.com

https://doi.org/10.37934/arfmts.107.1.190201

dimensional (2D) quasi-steady state analysis, and the resulting efficiency (η) increased by up to 20% (η becoming 87%). Cobb and Sharp [9] test results recommend that the pico scale Turgo turbine's angle of attack (α_1) is 20°. Warjito *et al.,* [2] utilized the curvature concept to design blades that can be manufactured using PVC pipes; follow-up research by Aaraj *et al.,* [10]. Aaraj *et al.,* [10] conceptualized the blade using the velocity triangle and elaborated on curvature; this proposal is difficult to manufacture in remote areas based on an engineering assessment by Warjito *et al.,* [2].

Saeed *et al.,* [6], Williamson *et al.,* [8], and Gaiser *et al.,* [11] explain the Turgo turbine performance (η) of 90%, 83%, and 91%, respectively; the performance is above 80% but use different geometries. Table 1 shows the details of the geometry. Table 1 shows no final agreement regarding the optimum parameter α_1, blade angle in the inlet (β_1), and outlet (β_2) for the pico scale Turgo turbine.

Table 1
Geometry of Turgo turbine blade and its performance in previous studies

Authors	α_1 (°)	β_1 (°)	β_2 (°)	ϒ (°)	P_{mech} (W)	η (%)
Gaiser *et al.,* [11]	30	79	19	11	83	90
Saeed *et al.,* [6]	20	34	30	56	85.98	83
Williamson *et al.,* [8]	20	60	30	20	89.69	91

Furthermore, several applied research was carried out to determine the reliability of the Turgo turbine at the pico scale with simple materials. The use of tablespoons for Turgo turbine blades to reduce manufacturing costs was proposed by Budiarso *et al.,* [12]. Budiarso *et al.,* [12] compared a tablespoon Turgo turbine with a Pelton turbine (precision blade). From an economic and performance, the Turgo turbine is more profitable than the Pelton turbine for the low-head [12]. Then, Adanta *et al.,* [13,14] utilized coconut shells as a Turgo turbine blade material, resulting in better performance than the Pelton turbine and Turgo turbine with a tablespoons blade.

The coconut shell does not have precise geometry, so the β_2 of each blade is different (although not significant). The Turgo turbine with coconut shell blade has better performance because it uses β_1 of 40° and α_1 of 20° which is the optimum condition based on analytical results [15]. Consequently, the difference β_2 of each blade is the wheel rotation looks unbalanced [13,14]; this condition should be avoided because it shortens generator life. Hence, the challenge for the Turgo turbine is how to manufacture precise, cheap, and fast blades. Three-dimensional (3D) printer technology is the suitable choice in Turgo turbine bade manufacturing to produce precise geometry, and fast. Therefore, this study aims to investigate the feasibility study of 3D printer technology to produce precise and fast Turgo turbine blades for pico scale.

2. Method

2.1 Analytical Method

Figure 1 shows the Turgo turbine design flowchart where a is the velocity triangle schematic, and b is the algorithm. From Figure 1, the specified boundary conditions are α_1, β_1, H, and Q. Magnitude of α_1 from 15° to 25°; this is to verify mathematically α_1 of 15° is optimum. Then, the β_1 of ~40° satisfies the U/C_{1x} of 0.5. Then, discharge (Q) of 2.5 lps and head (H) of 5 m is based on experimental or site conditions.

At inlet (Figure 1), H determines C_1, C_1 and α_1 for C_{1x} and C_{1r}, β_1 and C_{1r} for W_1. Then, W_1, C_1, and α_1 for U. At the outlet, the losses percentage due to shear between water to blade wall of 5%, expressed $W_2=0.95 \cdot W_1$. Further, U, W_2, and β_2 for determine C_2; β_2 are from 10° to 80°. Next, using trigonometry concepts, C_2, U, and W_2, for determining α2 and C2x.

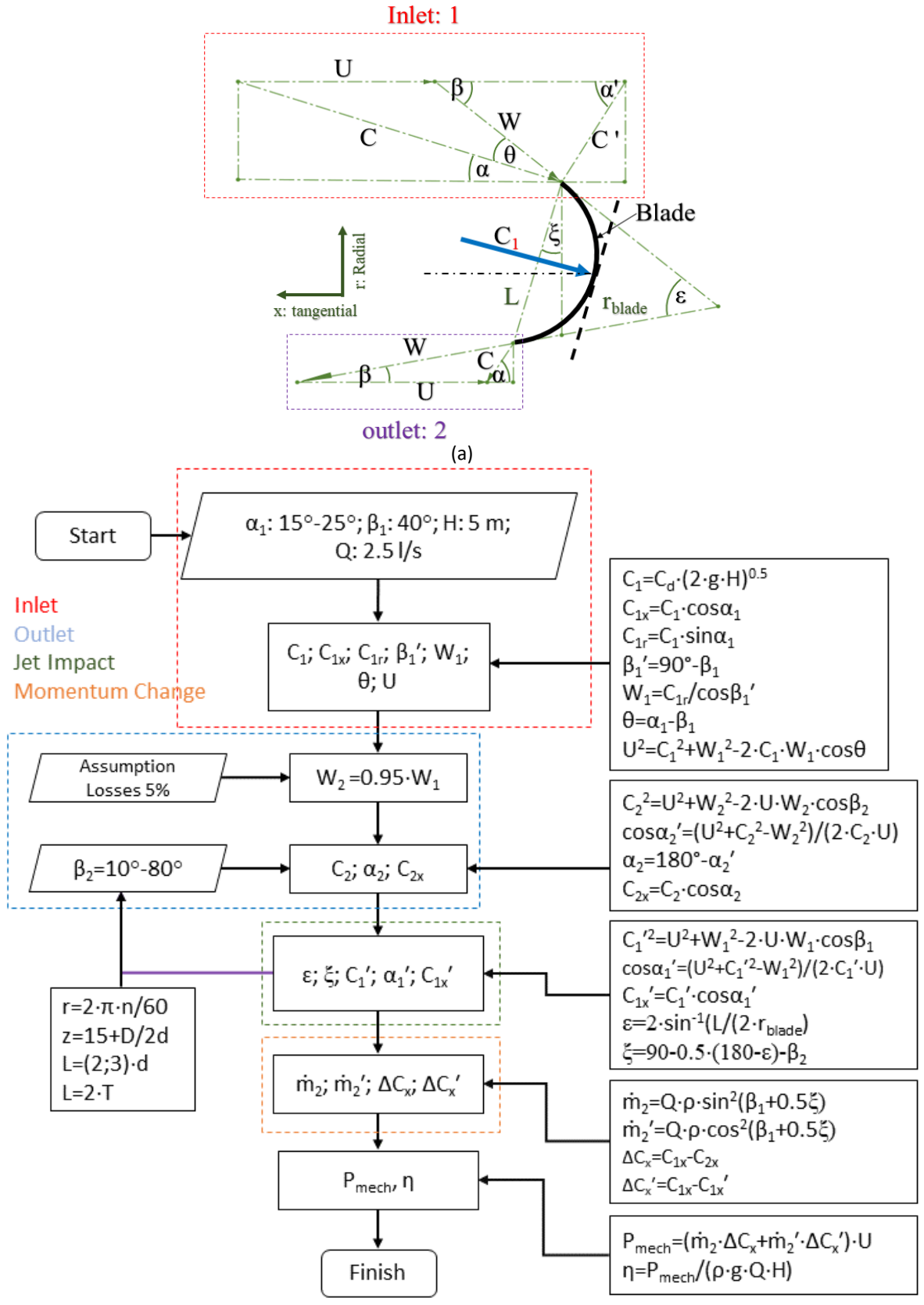

Fig. 1. Flow chart Turgo turbine design: (a) Velocity triangle schematic, (b) Algorithm

After the inlet and outlet are defined, the next step is to analyze the backflow, represented by C_1', C_{1x}', and α_1'. The backflow depicts the mass flow toward the inlet side ($\dot{m}_2'$). C_1' and α_1' are determined by W_1, U, and β_1 using the Pythagorean theorem. Then, using the trigonometry concept, C1x' is determined by C1' and α1'. The backflow is affected by the blade radius angle (ξ) and blade angle (ε); their formula can be seen in study by Syofii *et al.,* [16]. Therefore, the mass balance analysis is absorbed ($\dot{m}_2$) and considered as losses ($\dot{m}_2'$), which becomes

$$\dot{m}_2 = Q \cdot \rho \cdot \cos^2\left(\frac{90-\alpha_1-\xi}{2}\right) \tag{1}$$

$$\dot{m}_2' = Q \cdot \rho \cdot \sin^2\left(\frac{90-\alpha_1-\xi}{2}\right) \tag{2}$$

And the changes in velocity are ΔCx (energy extraction) and ΔCx' (losses)

$$\Delta C_x = C_{1x} - C_{2x} \tag{3}$$

$$\Delta C_x' = C_{1x} - C_{1x}' \tag{4}$$

Therefore, the mechanical power (P_{mech}) is adapted from the Euler equation and becomes

$$P_{mech} = \left(\dot{m}_2 \cdot \Delta C_x + \dot{m}_2' \cdot \Delta C_x'\right) \cdot U \tag{5}$$

Then, the Turgo turbine performance is a function of P_{mech} and P_{avai}, becomes

$$\eta = \frac{P_{mech}}{\rho \cdot g \cdot Q \cdot H} \times 100\% \tag{6}$$

The runner radius (r) is the geometry determined first using U=ω·r. Angular velocity (ω) is a function of wheel rotation (n). Then, determine the blade number (z) using z=15+(D/(2·d)); D is the wheel diameter, and d is the jet diameter. Rasio of d/D from 11 to 16 is optimum. Next, the calculation of blade radius (L) and blade depth (T) using L = (2;3)d, and T = 0.5L, respectively.

2.2 Experimental Method

The data logging system uses a microcontroller with an 8-bit capacity. Four instruments are used: a tachometer, DC current (I) and voltage (V) multimeter, and flowmeter. Determination of electric power (P_e) using

$$P_e = V \cdot I \tag{7}$$

Infrared sensor type E18-D80NK is used as a tachometer (measuring runner rotation). E18-D80NK sensor works by detecting objects and then reflecting light from infrared to the receptor. The amount of light reflected in unit time is processed by the microcontroller. The tachometer system using the E18-D80NK sensor has an uncertainty ($U_{0.95}$) of 0.04% and an error to the commercial device of 0.05%.

The discharge meter uses a YF-DN40 sensor mounted on a pipe with a diameter of 1.5 inches. YF-DN40 sensor specification is 0 to 150 lpm. The sensor consists of a valve body, water rotor and hall effect sensor. The YF-DN40 sensor activates when water flows through it, causing the rotor to rotate; the change in rotational speed is proportional to the discharge. Then, the hall effect sensor sends a pulse signal to the microcontroller, which processes it into discharge data measured in lpm. The flowmeter system using the YF-DN40 sensor has an error of 9.13%.

The multimeter is designed using the ACS 712 sensor to measure amperes and a 24V VCC sensor to measure direct voltage current (Vdc). The ACS712 sensor is a sensor capable of detecting AC and DC currents. This sensor has high accuracy by being supplied with 5V DC and 4.5V output voltage. Signals and voltages are sent to the microcontroller to be processed into currents and voltages to determine the measured DC power. Figure 2 depicts a schematic of the setup apparatus. The multimeter system using the ACS712 sensor has an uncertainty of 4.38% and using a 24V VCC sensor of 1.37%.

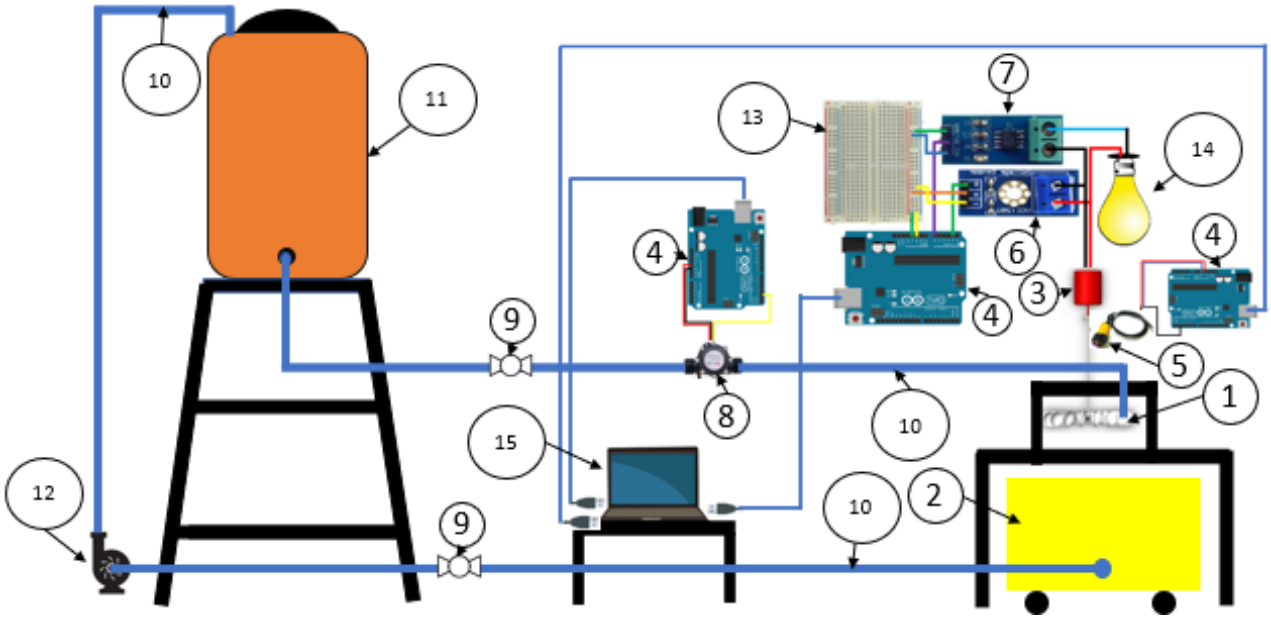

Fig. 2. Experimental setup of a pico-scale Turgo turbine

Information in Figure 2 is (1) Turgo turbine, (2) Reservoir, (3) DC Generators, (4) Arduino Uno, (5) E18-D80NK sensor, (6) ACS712 sensor, (7) 24V VCC sensor, (8) YF-DN40 sensor, (9) Valve, (10) Pipe, (11) Water tank, (12) Pump, (13) Writing Board, (14) Lights, and (15) Laptops

2.3 Blade Mechanical Strength Simulation Method

Mechanical strength simulation to predict acceptable Pp for blades using SOLIDWORKS for Students software. Figure 3 is a boundary condition set in the simulation, where the support is on the blade arm, and a static impact is applied to the blade. The static impact received by the blade is 100 N to 400 N.

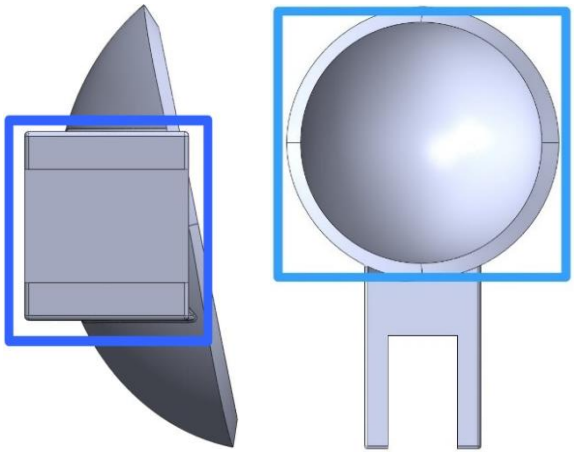

(a) (b)

Fig. 3. The boundary conditions of the mechanical strength simulation: (a) Support, (b) Static impact

3. Results and Discussion

3.1 Analytical Results

Figure 4(a) is the relationship between β_2 and α_1 to ΔC_x. From Figure 4, the higher the β_2, the smaller the ΔC_x. ΔC_x the smallest is at β_2 of 10° and α_1 of 25°. Based on Figure 4, the greater the β_2 and α_1, the greater the ΔC_x. Figure 4(b) is the relationship between β_2 and $\Delta C_x'$. From Figure 4(b), the relationship between β_2 and α_1 to $\Delta C_x'$ is linear; increasing β_2 and α_1 then $\Delta C_x'$ rising. The α_1 of 15° produces the lowest $\Delta C_x'$. Figure 4(c) is the relationship between β_2 to $\dot{m}_2$ and $\dot{m}_2'$. From Figure 4(c), the relationship between β_2 to $\dot{m}_2$ is inversely proportional to the relationship between β_2 to $\dot{m}_2'$. From the calculation results, the more significant the β_2, the $\dot{m}_2'$ increases and $\dot{m}_2$ decreases. The ratio of $\dot{m}_2$ and $\dot{m}_2'$ of 0.5 occurring at 20° β_2; the water energy is converted into mechanical energy and becomes losses has a ratio of 50%. Figure 4(d) is the relationship between α_1 and β_2 to τ, where their relationship is a parabola. Based on Figure 4(d), α_1 of 15° and 25° produces a lower τ than the others. Furthermore, α_1 of 20° has a higher τ than the others, where this condition occurs in all variations of β_2. Based on the calculation results, the smaller β_2 has a better τ than the larger β_2, and vice versa.

Figure 4(e) is the relationship of α_1 and β_2 to P_{mech}, where their relationship is a parabola. Figure 4(f) is the relationship between α_1 and β_2 to η. The pattern of the P_{mech} and η curves is similar to Figure 4(d) because it is influenced by $\dot{m}_2$ and $\dot{m}_2'$, which varies, while P_{avai} is constant. Table 2 shows the Turgo turbine blade dimensions obtained from the calculation results, and Figure 5 shows the Turgo turbine runner.

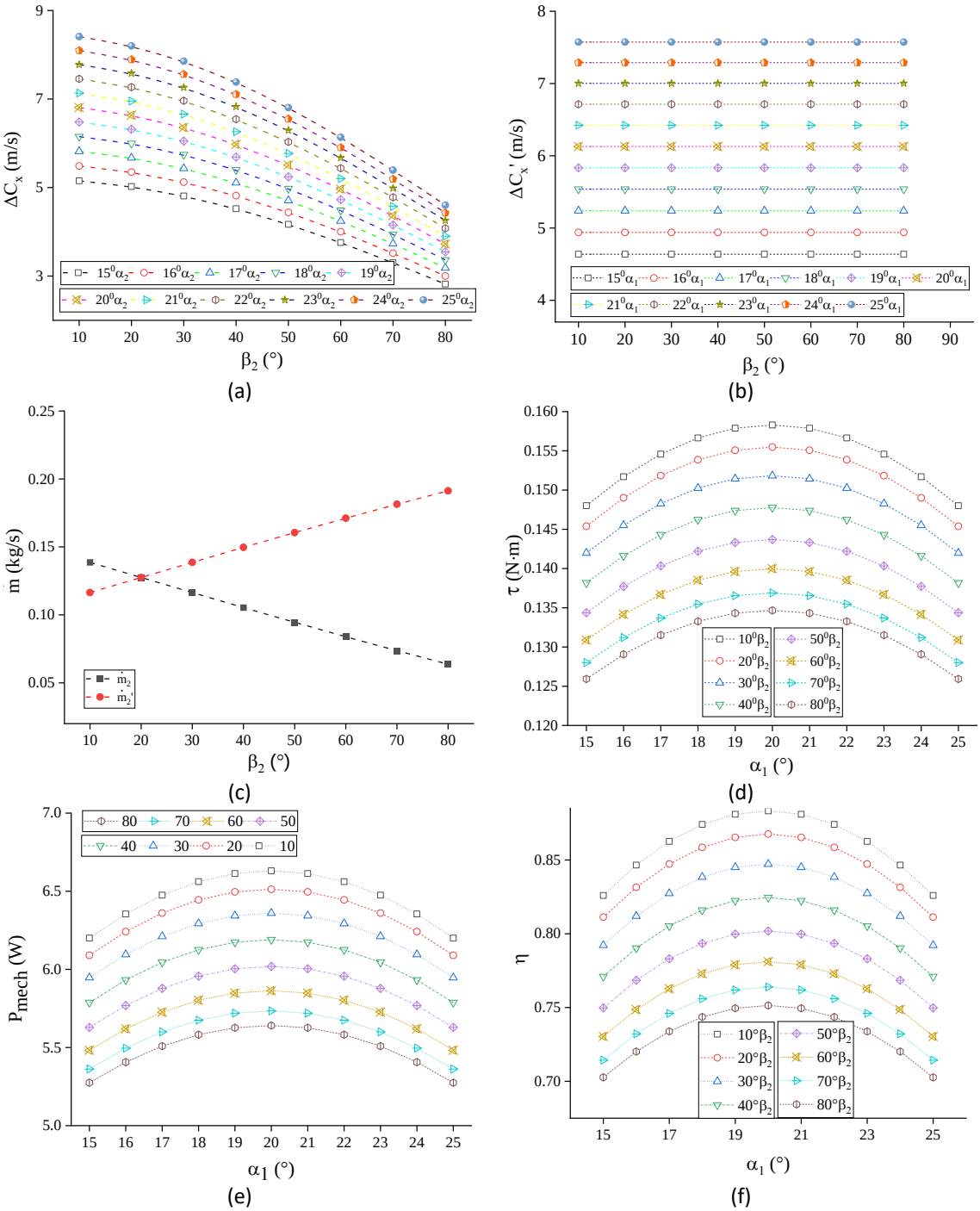

Fig. 4. Analytical results: (a) Relation of β_2 and α_1 to ΔC_x, (b) Relation of β_2 and α_1 with $\Delta C_x'$, (c) Relation of β_2 to $\dot{m}_2$ and $\dot{m}_2'$, (d) Relation of α_1 and β_2 to τ, (e) Relation of α_1 and β_2 to P_{mech}, and (f) Relation of α_1 and β_2 to η

Table 2
Turgo turbine blade dimensions calculated results

Parameters	Unit
β_1	40°
β_2	10°
α_1	20°
Z	16
r_{blade}	2.86 mm
D	274.53 mm
ξ	50°
ε	15°

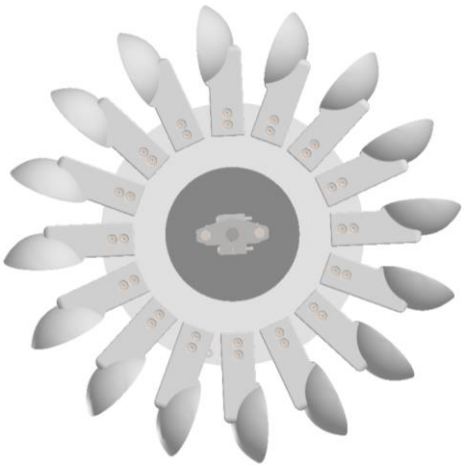

Fig. 5. Turgo turbine runner designed

3.2 Blade Mechanical Strength Simulation Results

The boundary conditions shall define the properties of the test material. Material properties similar to polylactic acid (PLA) with a maximum yield strength of 60 MPa are considered blade materials [1]. Static conditions mechanical strength tests are divided into Figure 6(a): 100 N, 150 N, 200 N, 250 N, 300 N, 350 N, 380 N, and 400 N. Visualization of the simulation of the results for 400 N in Figure 6(b).

Figure 6(a) is the result of a static mechanical strength simulation. From the simulation results, the maximum Von Mises load on the Turgo turbine scale pico blades designed using PLA material is 60 MPa. From Figure 6(a), the yield strength under loads of 390 N and 400 N exceeds the Von misses, which are 60.56 MPA and 62.11 MPa, respectively. Meanwhile, 380 N to 100 N loads yield strength does not exceed Von misses. Figure 6(b) is a visualization of the mechanical strength simulation results at a load of 400 N. Figure 6(b) shows blade areas with red conditions where the area is damaged.

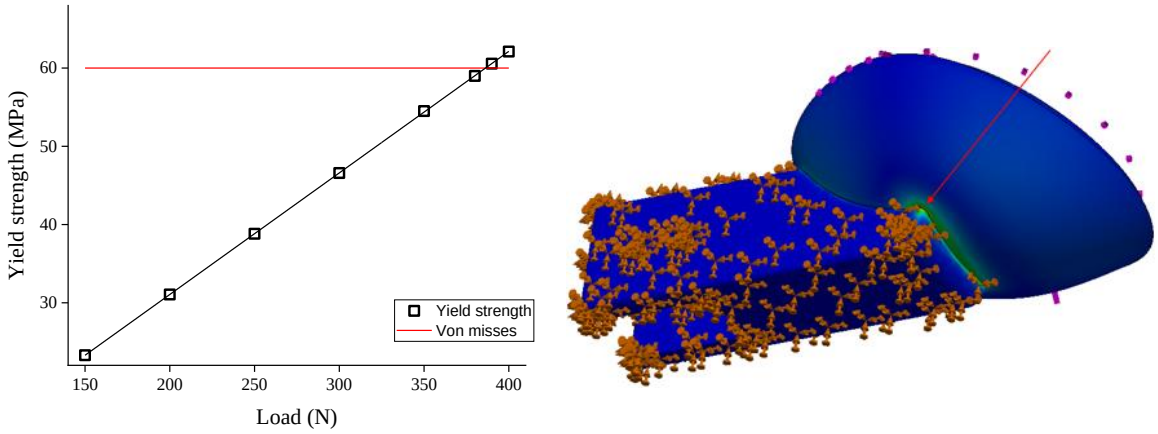

(a) (b)

Fig. 6. Mechanical strength simulation results: (a) Relation of load to yield strength, and (b) Visualization of 400 N load simulation results

Then, convert the load to P_{avai}. Table 3 is the result of converting the load into P_{avai}. From the conversion results (Table 3), P_{avai} that the blade can receive 17.5 W.

Table 3
Convert load to P_{avai}

F (N)	Q (lps)	Q (m^3/s)	H (C_1 1 m/s)	P_{avai} (W)
100	10	0.01	0.051	5
150	15	0.015	0.051	7.5
200	20	0.02	0.051	10
250	25	0.025	0.051	12.5
300	30	0.03	0.051	15
350	35	0.035	0.051	17.5
380	38	0.038	0.051	19

3.3 Experimental Results

Figure 7(a) shows the relation of P_{avai} to the absolute velocity of water (C_1) with the expression exponential. The experimental setup has the highest C_1 of 7.22 m/s with a P_{avai} of 14.81 W, the P_{avai} of the experimental setup is lower than that recommended by the mechanical strength simulation results.

Figure 7(b) shows the relation of n to V generated by the DC generator. From Figure 7(b), all variations in jet diameter (8, 9, 10 mm) increase in n and V. For a load of 1 lamp, the 9 mm jet produces the highest n of 329.67 rpm with a V of 9.87 V_{dc}. For a load of 2 lamps, a 10 m jet produces the highest n of 437.29 rpm with a V of 4.37 V_{dc}. Then, for 3 lamps, a 10 mm jet produces the highest n of 465.68 rpm with a V of 2.76 V_{dc}.

Figure 7(c) shows the relation of n to I generated by the DC generator. From Figure 7(c), all variations in jet diameter (8, 9, 10 mm) experience an increase in n and I, similar to the graph in Figure 7(b). For a load of 1 lamp, the 9 mm jet produces the highest n of 329.67 rpm with I of 87.8 mA. For a load of 2 lamps, a 10 m jet produces the highest n of 437.29 rpm with an I of 69.8 mA. Then, for 3 lamps, a 10 mm jet produces the highest n of 465.68 rpm with a V of 65.4 mA.

Figure 7(d) shows the relation of n to P_e, similar to Figure 7(b) and Figure 7(c). The patterns are similar because Pe is a function of V and I. Based on Figure 7(d), the highest P_e of 0.87 V_{dc} occurs at n of 329 rpm with 1 lamp load and 8 mm jet. Then, the lowest P_e of 0.08 Vdc occurred at n of 302.46 rpm with a load of 3 lamps and a 10 mm jet.

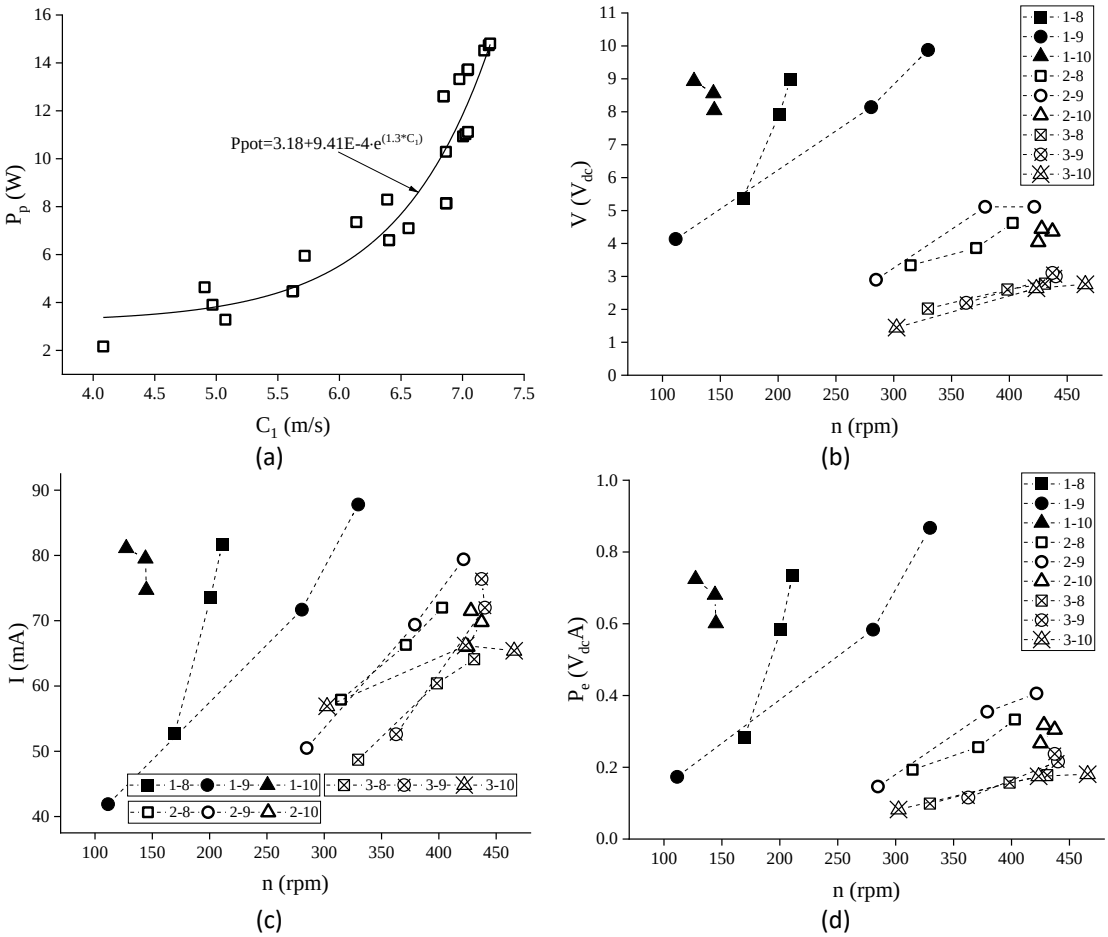

Fig. 7. Experimental results: (a) Relation of C_1 to P_{avai}, (b) Relation of n to V, (c) Relation of n to I, and (d) Relation of n to P_e

3.4 Discussion

Figure 8 shows a relation of the tip speed ratio (U/C_1) to the performance of the turbine (η), where the relationship is a parabola with an equation of the order 2. From Figure 8, the highest performance of the designed pico-scale Turgo turbine is 0.092 at U/C_1 of 0.5. The 0.5 U/C_1 showed similar test results to the Pelton Impulse turbine concept. Thus, the experimental test results can be said to be verified.

From the results of the velocity triangle analysis and experimental tests, the maximum conditions for the design of the pico-scale Turgo turbine blades are obtained. From the analytical results, α_1 is 20°, β_1 is 40°, β2 is 10°, r_{blade} is 15°. From the experimental results, the maximum η is 0.092 (9.2%), which is the electrical efficiency. Therefore, manufacturing pico-scale Turgo turbine blades using 3D printer technology is better than previous studies using coconut shells as the blade material [13]. Therefore, pico-scale printing of Turgo turbine blades using a 3D printing machine is recommended because of the ease of the manufacturing process, the time needed in the manufacturing process is short, and the cost is low.

Furthermore, from the results of calculations and experimental data, the average deviation between the analytical and experimental is 4%. Thus, the mathematical analysis using the velocity triangle approach has been verified and validated.

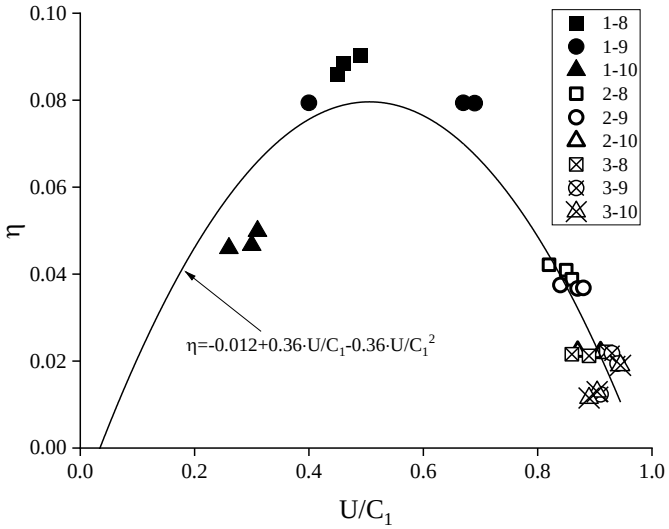

Fig. 8. Relation of U/C_1 to η

4. Conclusions

The Turgo turbine blade manufacturing method using 3D printer technology can be recommended because, from the mechanical strength simulation results, the maximum P_{avai} that can be received by Turgo turbine blades made from PLA is 17.5 W (35 lps). Then, from the experimental results, the maximum performance of the Turgo turbine made from PLA is 0.092 (9.2%). Furthermore, the geometry of the pico-scale Turgo turbine blades that produce maximum performance is as follows: α1 is 20°, β1 is 40°, β2 is 10°, r_{blade} is 15°.

Acknowledgement

The research/publication of this article was funded by DIPA of Public Service Agency of Universitas Sriwijaya 2022. SP DIPA-023.17.2.677515/2022, on December 13, 2021.

References

[1] Mizan, Muhammad, Warjito Warjito, Budiarso Budiarso, Ridho Irwansyah, Muhamad Agil Fadhel Kurnianto, and Muhammad Faridz Athaya. "The Performance of the Pico Scale Turgo Water Turbine Coconut Shell Blade with Variations in Nozzle Diameter and Distance." *Journal of Advanced Research in Fluid Mechanics and Thermal Sciences* 100, no. 1 (2022): 53-62. https://doi.org/10.37934/arfmts.100.1.5362

[2] Warjito, Warjito, Budiarso Budiarso, A. I. Siswantoro, Dendy Adanta, M. Kamal, and R. Dianofitra. "Simple bucket curvature for designing a low-head Turgo turbine for pico hydro application." *International Journal of Technology* 8, no. 7 (2017): 1239-1247. https://doi.org/10.14716/ijtech.v8i7.767

[3] Židonis, Audrius, David S. Benzon, and George A. Aggidis. "Development of hydro impulse turbines and new opportunities." *Renewable and Sustainable Energy Reviews* 51 (2015): 1624-1635. https://doi.org/10.1016/j.rser.2015.07.007

[4] Benzon, D. S., George Athanasios Aggidis, and J. S. Anagnostopoulos. "Development of the Turgo Impulse turbine: Past and present." *Applied Energy* 166 (2016): 1-18. https://doi.org/10.1016/j.apenergy.2015.12.091

[5] Warjito, Warjito, Alvi Arya Ramadhan, Budiarso Budiarso, Ridho Irwansyah, and Muhamad Agil Fadhel Kurnianto. "Performance Comparison of Straight, Curved, and Tilted Blades of Pico Scaled Vortex Turbine." *CFD Letters* 15, no. 2 (2023): 114-125. https://doi.org/10.37934/cfdl.15.2.114125

[6] Saeed, Ramiz Ibraheem, Ahmed Al-Manea, Ahmed Khalid Ibrahim, and Dendy Adanta. "Numerical Investigation on the Effect of Profile and Blade Numbers in a Savonius Vertical Axis Wind Turbine." *CFD Letters* 14, no. 9 (2022): 75-88. https://doi.org/10.37934/cfdl.14.9.7588

[7] Del Rio, Jorge Andrés Sierra, Alejandro Ruiz Sánchez, Daniel Sanín Villa, and Edwin Correa Quintana. "Numerical Study of H-Darrieus Turbine as a Rotor for Gravitational Vortex Turbine." *CFD Letters* 14, no. 8 (2022): 1-11. https://doi.org/10.37934/cfdl.14.8.111

[8] Williamson, Sam J., Bernard H. Stark, and Julian D. Booker. "Performance of a low-head pico-hydro Turgo turbine." *Applied Energy* 102 (2013): 1114-1126. https://doi.org/10.1016/j.apenergy.2012.06.029

[9] Cobb, Bryan R., and Kendra V. Sharp. "Impulse (Turgo and Pelton) turbine performance characteristics and their impact on pico-hydro installations." *Renewable Energy* 50 (2013): 959-964. https://doi.org/10.1016/j.renene.2012.08.010

[10] Aaraj, Youssef, Sorina Mortada, Denis Clodic, and Maroun Nemer. "Design Of A Turgo Two-Phase Turbine Runner." In *3rd International High Performance Buildings Conference*. 2014.

[11] Gaiser, Kyle, Paul Erickson, Pieter Stroeve, and Jean-Pierre Delplanque. "An experimental investigation of design parameters for pico-hydro Turgo turbines using a response surface methodology." *Renewable Energy* 85 (2016): 406-418. https://doi.org/10.1016/j.renene.2015.06.049

[12] Budiarso, Budiarso, Warjito Warjito, M. Naufal Lubis, and Dendy Adanta. "Performance of a low cost spoon-based turgo turbine for pico hydro installation." *Energy Procedia* 156 (2019): 447-451. https://doi.org/10.1016/j.egypro.2018.11.087

[13] Adanta, Dendy, Warjito Warjito, Dwijaya Febriansyah, and Budiarso Budiarso. "Feasibility analysis of a pico-scale turgo turbine bucket using coconut shell spoons for electricity generation in remote areas in Indonesia." *Journal of Advanced Research in Fluid Mechanics and Thermal Sciences* 69, no. 1 (2020): 85-97. https://doi.org/10.37934/arfmts.69.1.8597

[14] Adanta, Dendy, Imam Syofii, Dewi Puspita Sari, and Apri Wiyono. "Performance of Pico Scale Turgo Turbine in Difference the Nozzle Diameter." *International Journal of Fluid Machinery and Systems* 15, no. 1 (2022): 130-136. https://doi.org/10.5293/IJFMS.2022.15.1.130

[15] Anagnostopoulos, John S., Phoevos K. Koukouvinis, Fotis G. Stamatelos, and Dimitris E. Papantonis. "Optimal design and experimental validation of a Turgo model Hydro turbine." In *Engineering Systems Design and Analysis*, vol. 44854, pp. 157-166. American Society of Mechanical Engineers, 2012. https://doi.org/10.1115/ESDA2012-82565

[16] Syofii, Imam, Andre Brilian Hidayatullah, Dendy Adanta, Dewi Puspita Sari, Firmansyah Burlian, and Muhammad Amsal Ade Saputra. "Pico Scale Turgo Turbine Design for Remote Areas Application Using Velocity Triangle Approach." *Journal of Advanced Research in Fluid Mechanics and Thermal Sciences* 97, no. 1 (2022): 157-167. https://doi.org/10.37934/arfmts.97.1.157167